Dileptons from P-Nucleus Collisions

Jen-Chieh Peng

Physics Division, Los Alamos National Laboratory
Los Alamos, New Mexico 87545

Abstract. Recent results from fixed-target dimuon production experiments at Fermilab are presented. Various QCD tests using dilepton production data are discussed. We emphasize that clear evidence for scaling violation in the Drell-Yan process remains to be established. Further theoretical and experimental work are needed to understand the polarization of the Drell-Yan pairs. We also discuss the nuclear medium effects for dilepton productions. In particular, we discuss the use of Drell-Yan data to deduce the energy-loss of partons traversing nuclear medium.

INTRODUCTION

The experimental detection of high-mass lepton pairs produced in hadronic reactions has a long and rich history. The famous quarkonium states that revealed the existence of the charm and beauty quarks in the 1970s were discovered through their dilepton decay branches. They are superimposed on a continuum, which was anticipated theoretically in 1970 [1], and is now known as the Drell-Yan (DY) process. The DY process, electromagnetic quark-antiquark annihilation, is closely related to the deeply inelastic lepton scattering (DIS). By 1980, DY production was already a source of information about antiquark structure of the nucleon. Additionally, DY production with beams of pions and kaons yielded the structure functions of these unstable particles for the first time. Also notable in the history of the DY process were the discoveries of the $W^{\pm}$ and Z^0 particles in 1983, produced by a generalized (vector boson exchange) quark-antiquark annihilation mechanism.

New experimental work has been carried out in recent years by few but prolific collaborations working in the fixed-target programs at the CERN SPS accelerator and at Fermilab. A series of fixed-target dimuon production experiments (E772, E789, E866) have been carried out at Fermilab in the last 10 years. Some of the highlights from these experiments, namely the observation of pronounced flavor asymmetry in the nucleon sea and the absence of antiquark enhancement in heavy nuclei, are discussed by Garvey at this Conference. In this paper, we will focus on other areas of dilepton physics studied in these experiments. To follow the main theme of this Conference, we first discuss the status of various QCD tests using

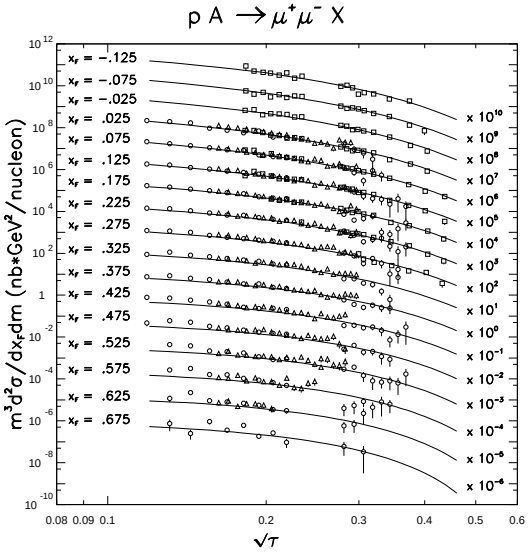

FIGURE 1. Proton-induced Drell-Yan production from experiments NA3 [2] (triangles) at 400 GeV/c, E605 [3] (squares) at 800 GeV/c, and E772 [4] (circles) at 800 GeV/c. The lines are absolute (no arbitrary normalization factor) next-to-leading order calculations for $p+d$ collisions at 800 GeV/c using the CTEQ4M structure functions [5].

dilepton productions. We will then discuss the nuclear medium effects for dilepton productions. In particular, the relevance of the Fermilab experiments on the issue of parton energy loss in nuclei will be presented.

QCD TESTS IN DILEPTON PRODUCTION

In the "Naive" Drell-Yan model, the differential cross section is given as

$$M^3 \frac{d^2\sigma}{dMdx_F} = \frac{8\pi\alpha^2}{9} \frac{x_1 x_2}{x_1 + x_2} \times \sum_a e_a^2 [q_a(x_1)\bar{q}_a(x_2) + \bar{q}_a(x_1)q_a(x_2)]. \qquad (1)$$

Here $q_a(x)$ are the quark or antiquark structure functions of the two colliding hadrons evaluated at momentum fractions x_1 and x_2. The sum is over quark flavors. The Feynman-x (x_F) is equal to $x_1 - x_2$.

Although the simple parton model originally proposed by Drell and Yan enjoyed considerable success in explaining many features of the early data, it was soon realized that QCD corrections to the parton model were required. Historically, two experimental features demanded theoretical improvement: first, the experimental cross section was about a factor of two larger than the parton-model value, and second, the distribution of dilepton transverse momenta extended to much larger values than are characteristic of the convolution of intrinsic parton momenta. We now discuss several consequences of QCD corrections to the DY observables.

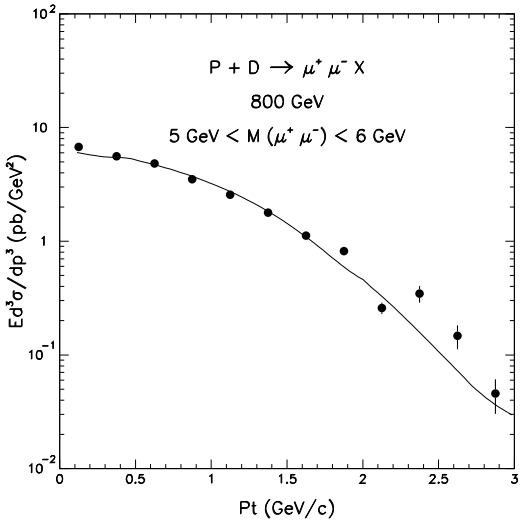

FIGURE 2. Comparison between the NLO calculation from Ref. [6] and the E772 data [4].

Absolute Cross Sections and p_T Distribution

The inclusion of the NLO diagrams for the DY process brings excellent agreements between the calculations and the data. As an example, Figure 1 shows the NA3 data [2] at 400 GeV, together with the E605 [3] and E772 [4] data at 800 GeV. The solid curve in Figure 1 corresponds to NLO calculation for 800 GeV $p+d$ ($\sqrt{s}$ = 38.9 GeV) and it describes the NA3/E605/E772 data well.

Berger et al. [6] recently compared their NLO calculations with the E772 data. As shown in Figure 2, the p_T distribution is well reproduced by the calculation. At $p_T > 2$ GeV/c, the DY cross section is shown to be dominated by processes involving gluons. This suggests the interesting possibility of probing gluon density using large p_T DY events.

Scaling Violation

The right-hand side of Eq. (1) is only a function of x_1, x_2 and is independent of the beam energies. This scaling property no longer holds when QCD corrections to the DY are taken into account.

While logarithmic scaling violation is well established in DIS experiments, it is not well confirmed in DY experiments at all. No evidence for scaling violation is seen. As discussed in a recent review [7], there are mainly two reasons for this. First, unlike the DIS, the DY cross section is a convolution of two structure functions. Scaling violation implies that the structure functions rise for $x \leq 0.1$ and drop for $x \geq 0.1$ as Q^2 increases. For proton-induced DY, one often involves a beam quark with $x_1 > 0.1$ and a target antiquark with $x_2 < 0.1$. Hence the effects of scaling

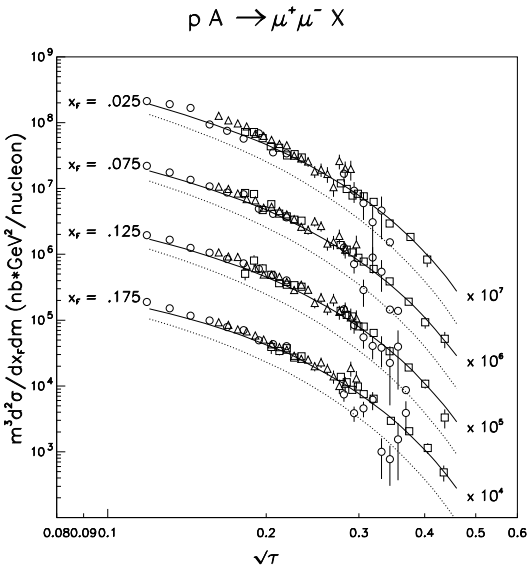

FIGURE 3. Comparison of DY cross section data with NLO calculations using MRST [10] structure functions. Note that $\tau = x_1 x_2$. The E772 [4], E605 [3], and NA3 [2] data points are shown as circles, squares, and triangles, respectively. The solid curve corresponds to fixed-target p+d collision at 800 GeV, while the dotted curve is for p+d collision at $\sqrt{s} = 500$ GeV.

violation are partially cancelled. Second, unlike the DIS, the DY experiment can only probe relatively large Q^2, namely, $Q^2 > 16$ GeV^2 for a mass cut of 4 GeV. This makes it more difficult to observe the logarithmic variation of the structure functions in DY experiments.

Possible indications of scaling violation in DY process have been reported in two pion-induced experiments, E326 [8] at Fermilab and NA10 [9] at CERN. E326 collaboration compared their 225 GeV $\pi^- + W$ DY cross sections against calculations with and without scaling violation. They observed better agreement when scaling violation is included. This analysis is subject to the uncertainties associated with the pion structure functions, as well as the nuclear effects of the W target. The NA10 collaboration measured $\pi^- + W$ DY cross sections at three beam energies, namely, 140, 194, and 286 GeV. By checking the ratios of the cross sections at three different energies, NA10 largely avoids the uncertainty of the pion structure functions. However, the relatively small span in $\sqrt{s}$, together with the complication of nuclear effects, make the NA10 result less than conclusive.

RHIC provides an interesting opportunity for unambiguously establishing scaling violation in the DY process. Figure 3 shows the predictions for $p + d$ at $\sqrt{s} =$ 500 GeV. The scaling-violation accounts for a factor of two drop in the DY cross sections when $\sqrt{s}$ is increased from 38.9 GeV to 500 GeV. It appears quite feasible to establish scaling violation in DY with future dilepton production experiments at RHIC.

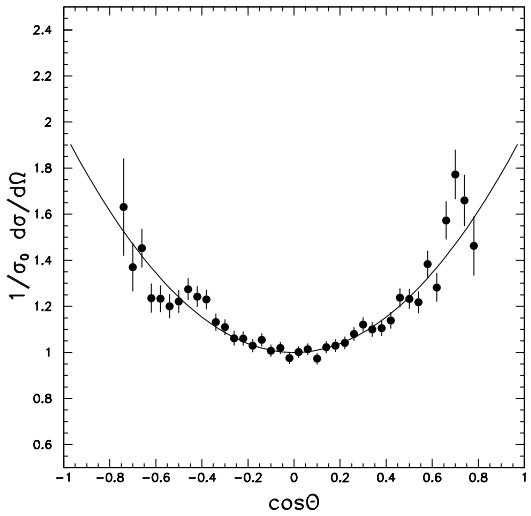

FIGURE 4. Drell-Yan angular distribution from Fermilab E772 [12]: $p + Cu$ collisions at 800 GeV/c. The dimuons cover the mass region $11 \leq M_{\mu^+\mu^-} \leq 17$ GeV/c^2 with $-0.3 \leq x_F \leq 0.8$ and $p_t \leq 6$ GeV/c. Mean values for p_t, x_F, and M are 1.4 GeV/c, 0.16, and 11.9 GeV/c^2, respectively. The solid curve is a fit to the data with the form $1 + \lambda cos^2\theta$, where λ is $0.96 \pm .04 \pm .06$.

Decay Anugular Distributions

In the parton model, the angular distribution of dileptons is characteristic of the decay of a transversely polarized virtual photon,

$$\frac{d\sigma}{d\Omega} = \sigma_0(1 + \lambda cos^2\theta), \tag{2}$$

where θ is the polar angle of the lepton in the virtual photon rest frame and $\lambda = 1$. Early experimental data from both pion and proton beams [11] were consistent with this form but had large statistical errors.

Recently, E772 has performed a high-statistics study of the angular distribution for DY events [12] with masses above the Υ family of resonances. About 50,000 events were recorded from 800 GeV/c $p + Cu$ collisions, using a copper beam dump as the target. Figure 4 shows the acceptance-corrected angular distribution, integrated over the kinematic variables. Analyzed in the Collins-Soper reference frame [13], the data yield $\lambda = 0.96 \pm 0.04 \pm 0.06$(systematic).

Including higher-order QCD corrections to the DY process [14,15] results in the more complicated form of the angular distribution,

$$\frac{d\sigma}{d\Omega} \propto 1 + \lambda cos^2\theta + \mu sin2\theta cos\phi + \frac{\nu}{2} sin^2\theta cos2\phi, \tag{3}$$

where ϕ is the azimuthal angle and λ, μ, and ν are angle-independent parameters. NLO calculations predict [16] small deviations from $1 + cos^2\theta$ ($\leq 5\%$) for p_t below

3 GeV/c. The relevant scaling parameter for the magnitude of these deviations is p_t/Q, implying that NLO corrections become important when $p_t \simeq Q$. A relation, $1 - \lambda - 2\nu = 0$, developed by Lam & Tung [17], is analogous to the Callan-Gross relation in DIS. Measurements with pion beams at CERN [18] and at Fermilab [19] have shown that the Lam-Tung relation is clearly violated at large p_t.

Pion-induced DY experiments have unexpectedly shown that transverse photon polarization changes to longitudinal ($\lambda \simeq -1$) at large x_F [18–21]. The x_F dependence of λ is qualitatively consistent with a higher-twist model originally proposed by Berger & Brodsky [22,23]. However, the quantitative agreement is poor. The model's basis can be described as follows. As x_F of the muon pair approaches unity, the Bjorken-x (momentum fraction) of the annihilating projectile parton must also be near unity. Thus, the whole pion contributes to the DY process. This can be treated with perturbation theory, with the result that the transverse polarization of the virtual photon becomes longitudinal. The angular distribution at large x_F becomes

$$\frac{d\sigma}{d\Omega} \propto (1-x)^2(1 + \lambda cos^2\theta) + \alpha sin^2\theta, \tag{4}$$

where α is $\propto p_t^2/Q^2$.

Eskola et al [24] have shown that an improved treatment of the effects of nonasymptotic kinematics greatly improves quantitative agreement with the λ values from the pion data. Brandenburg et al [25] have extended the higher twist model to specifically include pion bound-state effects. They predict values for λ, μ and ν that are in good agreement with the pion data at large x_F. Unfortunately, the results are quite sensitive to the choice of the pion Fock state wave functions, which are not well constrained by experimental data.

NUCLEAR MEDIUM EFFECTS OF DILEPTON PRODUCTION

From a high-statistics measurement of dilepton production in 800 GeV proton-nucleus interaction, the target-mass dependence of DY, J/Ψ, Ψ', and Υ productions have been determined in E772 [26–28]. As shown in Figure 5, different nuclear dependences are observed for different dilepton processes. While the DY process shows almost no nuclear dependence, pronounced nuclear effects are seen for the production of heavy quarkonium states. E772 found that J/Ψ and Ψ' have similar nuclear dependence. The nuclear dependences for Υ, Υ' and Υ'' are less than that observed for the J/Ψ and Ψ'. Within statistics, the various Υ resonances also have very similar nuclear dependences.

Although the integrated DY yields in E772 show little nuclear dependence, it is instructive to examine the DY nuclear dependences on various kinematic variables. Using the simple A^α expression to fit the DY nuclear dependence, the values of α

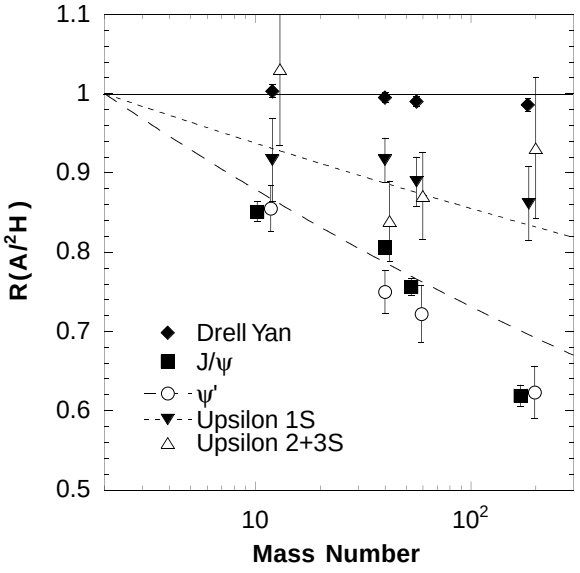

FIGURE 5. Ratios of heavy-nucleus to deuterium integrated yields per nucleon for 800 GeV proton production of dimuons from the Drell-Yan process and from decays of the J/ψ, ψ', $\Upsilon(1S)$, and $\Upsilon(2S+3S)$ states [7]. The short dash and long dash curves represent the approximate nuclear dependences for the $b\bar{b}$ and $c\bar{c}$ states, $A^{0.96}$ and $A^{0.92}$, respectively.

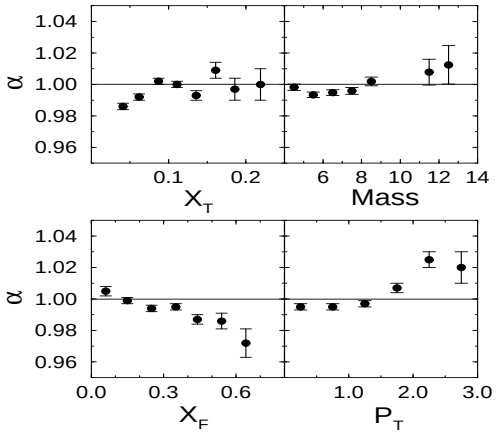

FIGURE 6. Nuclear dependence coefficient α for 800 GeV p+A Drell-Yan process versus various kinematic variables [26].

are shown in Figure 6 as a function of $x_T(x_2)$, M, x_F, and p_t. Several features are observed:

1. A suppression of the DY yields from heavy nuclear targets is seen at small x_2. This is consistent with the shadowing effect observed in DIS. In fact, E772 provides the only experimental evidence for shadowing in hadronic reactions. The reach of small x_2 in E772 is limited by the mass cut ($M \geq 4$ GeV) and by the relatively small center-of-mass energy (recall that $x_1 x_2 = M^2/s$). p-A collisions at RHIC clearly offer the exciting opportunity to extend the study of shadowing to much smaller x.

2. $\alpha(x_F)$ shows an interesting trend, namely, it decreases as x_F increases. It is tempting to attribute this behavior to initial-state energy-loss effect. However, there is a strong correlation between x_F and x_2 ($x_F = x_1 - x_2$), and it is essential to separate the x_F energy-loss effect from the x_2 shadowing effect. Figure 7 shows α versus x_F for two bins of x_2, one in the shadowing region ($x_2 \leq 0.075$) and one outside of it ($x_2 \geq 0.075$). There is no discernible x_F dependence for α once one stays outside of the shadowing region. Therefore, the apparent suppression at large x_F in Figure 6 reflects the shadowing effect at small x_2 rather than the energy-loss effect.

3. $\alpha(p_t)$ shows an enhancement at large p_t. This is reminiscent of the Cronin Effect [29] where the broadening in p_t distribution is attributed to multiple parton-nucleon scatterings. It is instructive to compare the p_t broadening for DY process and quarkonium production. Figure 8 shows $\Delta\langle p_t^2\rangle$, the difference of mean p_t^2 between p-A and p-D interactions, as a function of A for DY, J/Ψ, and $\Upsilon(1S)$ productions at 800 GeV. The DY and Υ data are from E772 [30], while the J/Ψ results are from E789 [31], E771 [32], and preliminary E866 analysis [33]. More details on this analysis will be presented elsewhere [30]. Figure 8 shows that $\langle p_t^2\rangle$ is well described by the simple expression $a+bA^{1/3}$. It also shows that the p_t broadening for J/Ψ is very similar to Υ, but significantly larger (by a factor of 5) than the DY. A factor of 9/4 could be attributed to the color factor of the initial gluon in the quarkonium production versus the quark in the DY process. The remaining difference could come from the final-state multiple scattering effect which is absent in the DY process.

Baier et al. [34] have recently derived a relationship between the partonic energy-loss due to gluon bremsstrahlung and the mean p_t^2 broadening accumulated via multiple parton-nucleon scattering:

$$-dE/dz = \frac{3}{4}\,\alpha_s\,\Delta\langle p_t^2\rangle. \tag{5}$$

This non-intuitive result states that the total energy loss is proportional to square of the path length traversed by the incident partons. From Figure 8 and Eq. 5, we deduce that the mean total energy loss, ΔE, for the p+W DY process is ≈ 0.6

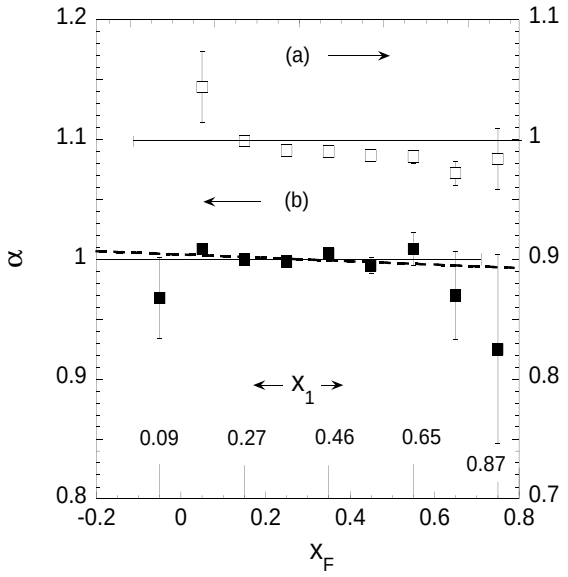

FIGURE 7. Nuclear dependence coefficient α for the Drell-Yan process [26] versus x_F for (a) $x_2 \leq 0.075$, right scale, and (b) $x_2 \geq 0.075$, left scale. The thin solid lines show $\alpha = 1$. The dashed line is a linear least-squares fit to the lower points. Also shown is the mean value of x_1 for (b).

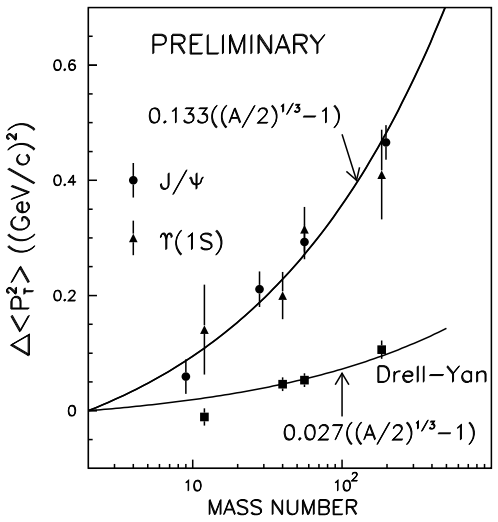

FIGURE 8. The change of mean p_t^2 for nuclear target, $\Delta\langle p_t^2\rangle = \langle p_t^2\rangle(A) - \langle p_t^2\rangle(D)$, for 800 GeV p+A Drell-Yan process and J/Ψ and $\Upsilon(1S)$ productions. The solid curves are best fits to the A-dependence of $\Delta\langle p_t^2\rangle$. The J/Ψ and $\Upsilon(1S)$ productions have identical curves for the A-dependence fits.

GeV. Such an energy-loss is too small to cause any discernible effect in the x_F (or x_1) nuclear dependence. As shown in Figure 7, the dashed curve corresponds to $\Delta E = 2.0 \pm 1.7$ GeV (for p+W), and the E772 data are consistent with Eq. 5. A much more sensitive test for Eq. 5 could be done at RHIC, where the energy-loss effect is expected to be much enhanced in A-A collision [35].

REFERENCES

1. Drell S. D., and Yan T. M., *Phys. Rev. Lett.* **25**, 316 (1971).
2. Badier J. et al., *Z. Phys.* **C26**, 489 (1984).
3. Moreno G. et al., *Phys. Rev.* **D43**, 2815 (1991).
4. McGaughey P. L. et al., *Phys. Rev.* **D50**, 3038 (1994).
5. Lai H. L. et al., *Phys. Rev.* **D55**, 1280 (1997).
6. Berger E. L., Gordon L. E., and Klasen M., *Phys. Rev.* **D58**, 074012 (1998).
7. McGaughey P. L., Moss J. M., and Peng J. C., hep-ph/9905409, to be published in *Annu. Rev. Nucl. Part. Sci.* (1999).
8. Greenlee H. B. et al., *Phys. Rev. Lett.* **55**, 1555 (1985).
9. Freudenreich K., *Int. J. Mod. Phys.* **A5**, 3643 (1990).
10. Martin A. D. et al., *Eur. Phys. J.* **C4**, 463 (1998).
11. Kenyon I. R., *Rep. Prog. Phys.* **45**, 1261 (1982).
12. McGaughey P. L., *Nucl. Phys.* **A610**, 394c (1996).
13. Collins J. C., and Soper D. E., *Phys. Rev.* **D16**, 2219 (1977).
14. Oakes R. J., *Nuovo Cim.* **A44**, 440 (1966).
15. Collins J. C., *Phys. Rev. Lett.* **42**, 291 (1979).
16. Chiappetta P., and Le Bellac M., *Z. Phys.* **C32**, 521 (1986).
17. Lam C. S., and Tung W. K., *Phys. Rev.* **D21**, 2712 (1980).
18. Guanziroli M et al., *Z. Phys.* **D37**, 545 (1988) .
19. Conway J. S. et al., *Phys. Rev.* **D39**, 92 (1989).
20. Badier J. et al., *Z. Phys.* **C11**, 195 (1981).
21. Heinrich J. G. et al., *Phys. Rev.* **D44**, 1909 (1991)
22. Berger E. L., and Brodsky S. J., *Phys. Rev. Lett.* **42**, 940 (1979).
23. Berger E. L., *Z. Phys.* **C4**, 289 (1980).
24. Eskola K. J. et al., *Phys. Lett.* **B333**, 526 (1994).
25. Brandenburg A et al., *Phys. Rev. Lett.* **73**, 939 (1994).
26. Alde D. A., et al., *Phys. Rev. Lett.* **64**, 2479 (1990).
27. Alde D. A. et al., *Phys. Rev. Lett.* **66**, 133 (1991).
28. Alde D. A. et al., *Phys. Rev. Lett.* **66**, 2285 (1991).
29. Cronin J. W. et al., *Phys. Rev.* **D11**, 3105 (1975).
30. McGaughey P. L., Moss J. M., and Peng J. C., to be published (1999).
31. Schub M. H. et al., *Phys. Rev.* **D52**, 1307 (1995).
32. Alexopoulos T. et al., *Phys. Rev.* **D55**, 3927 (1997).
33. Leitch M. J., in Proceedings of "Quarkonium Production in Relativistic Nuclear Collisions", Institute for Nuclear Theory, Seattle, WA, May 1998.

34. Baier R. et al., *Nucl. Phys.* **B484**, 265 (1997); Baier R. et al., *Nucl. Phys.* **B531**, 403 (1998).
35. Baier R. et al., *Nucl. Phys.* **B483**, 291 (1997).